CONTROL METHODS FOR ACTIVE POWER FILTERS WITH MINIMUM MEASUREMENT REQUIREMENTS

Domenico Casadei, Gabriele Grandi, Ugo Reggiani, Claudio Rossi

Dept. of Electrical Engineering, University of Bologna
viale Risorgimento 2, I-40136, Bologna - Italy
E-mail: elettrot5@dns.ing.unibo.it

Abstract - Two shunt active power filter configurations are analyzed in this paper in order to define new control methods characterized by simple control algorithms and minimum voltage and current transducer requirements. The transfer functions for the two control schemes are determined and analyzed to emphasize the active filter behavior in both steady-state and transient conditions. The performance obtained by the proposed control schemes is similar to that of standard solutions. The experimental results substantially confirm the numerical results obtained by Simulink of Matlab.

I. INTRODUCTION

Parallel active filters have been recognized as a valid solution to current harmonic and reactive power compensation of non-linear loads. As it is known, the principle of operation is based on the injection of the current harmonics required by the load. As a consequence, the characteristics of the harmonic compensation are strongly dependent on the filtering algorithm employed for the calculation of load current harmonics. Various active power filter configurations and control strategies have been proposed and developed in the last decade [1]-[8]. The performance of any configuration is dependent on the method employed to implement the current regulator. Hysteresis current regulators have been extensively used for active filter applications because of their wide bandwidth and simple structure. Alternatively, the implementation of current regulators can be realized by PWM-controlled Voltage Source Inverter (VSI) [9]-[14]. Regardless of the type of current regulator, two current measurement systems are usually employed in active filters to sense the load and filter currents. Furthermore, powerful microprocessors are necessary for the on-line evaluation of the harmonic content of the load currents.

In order to simplify the control scheme, two active power filter configurations are proposed in this paper. The corresponding block diagrams are represented in Figs. 1 and 2. They are based on a single current measurement system and the current regulation is achieved by using a PWM-controlled VSI. The control scheme of Fig. 1 needs the measurement of the source current only, whereas the control scheme of Fig. 2 needs the measurement of the load current only.

Both active filter configurations are based on the same principle, which consists in the direct generation of reference values for the source current on the basis of the dc-voltage level. According to this principle, the current regulator acts in order to force the source currents to be sinusoidal and in phase with the corresponding line-to-neutral voltages. In this way, the need of manipulating the load currents to extract the harmonic components can be avoided.

The two control schemes are analyzed and compared through the Simulink tool of Matlab. The numerical simulations are validated by experimental results.

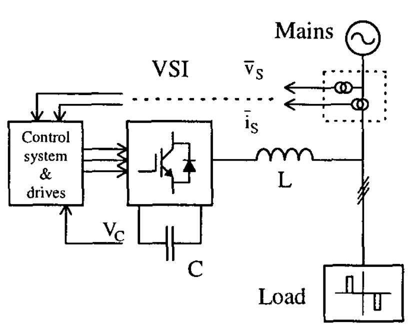

Fig. 1. Active power filter with source current measurement only.

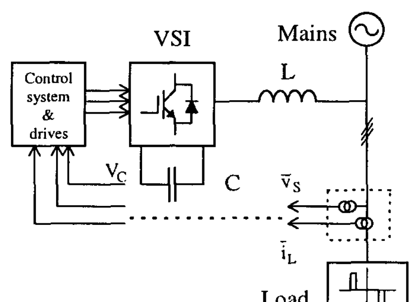

Fig. 2. Active power filter with load current measurement only.

This work was partially supported by E.U. INCO-COPERNICUS Project PL 962063

II. PRINCIPLE OF OPERATION

As it is known, active power filters are used for compensating reactive power and low-order current harmonics generated by non-linear loads. The maximum harmonic order that an active filter is able to compensate determines the filter bandwidth. As a result of the active filter operation, the source currents become almost sinusoidal with unity power factor. Most of the solutions proposed to implement the control system are based on the measurement of both the load and filter currents. The source voltage measurement is also required for the synchronization of the inverter output voltages or for coordinate transformations, depending on the employed control strategy. In this paper, the possibility of using active filters operating with a single current measurement system is investigated [15]-[17]. Depending on whether the source currents or the load currents are measured, the block diagram shown in Fig. 1 and Fig. 2, respectively, must be considered. In these figures and in the continuation of the paper, three-phase quantities are represented with space vectors according to a stationary d-q transformation.

The proposed schemes have been implemented using the same basic principle, i.e. the generation of a reference value for the source current $\bar{i}_S^*$ in phase with the source voltage $\bar{v}_S$, as represented in Fig. 3. The magnitude of the reference source current I_S^* is obtained applying the regulator $R(s)$ to the instantaneous error between the reference dc-link voltage V_C^* and the actual dc-link voltage V_C measured across the capacitor C. I_S^* is then modulated by the unity source voltages to generate the reference value for the source currents.

III. ANALYSIS OF THE DYNAMIC BEHAVIOR

In this section, the active filter configurations shown in Figs. 1 and 2 are analyzed and compared. It can be noted that the system performance is dependent on the time responses of the ac current controller and dc-link voltage regulator. However, the dynamic behavior of the filter is mainly affected by the time response of the ac current control loop, which must be designed in order to track the reference current waveforms closely. The dc voltage control loop has the task to keep the dc voltage level close to its reference value and may not be very fast. A frequency analysis can be carried out with reference to the simplified block diagram represented in Fig. 4. In this diagram, the input of the regulator $R(s)$ is the error of the capacitor stored energy, the output is the reference value of the source power P_S^* defined as $P_S^* = V_S I_S^*$. The reference value of the power absorbed by the filter P_F^* is calculated by subtracting the load power P_L to P_S^*. Assuming that the VSI is able to generate the reference power at each cycle period yields $P_F = P_F^*$. This instantaneous power represents the total power flowing from the supply to the active filter. Neglecting the rate of change of the magnetic energy in the ac-link inductors, P_F represents the input power of the VSI. Furthermore, being negligible the losses of the converter, the energy stored in the capacitor E_C is given by the time integral of P_F. Under these assumptions, the following expression can be derived from the block diagram represented in Fig. 4

$$E_C = \frac{R(s)}{s+R(s)} E_C^* - \frac{1}{s+R(s)} P_L . \tag{1}$$

The choice of the regulator $R(s)$ should be made taking the desired active filter performance into account. A detailed discussion on different types of regulators is given in [18]. In order to obtain a zero steady-state error, the regulator must introduce an integral action. Then, choosing for $R(s)$ a PI regulator expressed as

$$R(s) = K_p\left(1+\frac{1}{T_i s}\right) = K_p \frac{1+T_i s}{T_i s} \tag{2}$$

leads to

$$E_C = \frac{\omega_n^2(1+T_i s)}{s^2+2\delta\omega_n s+\omega_n^2} E_C^* - \frac{s}{s^2+2\delta\omega_n s+\omega_n^2} P_L , \tag{3}$$

where $\omega_n = \sqrt{\frac{K_p}{T_i}}$ and $\delta = \frac{1}{2}\sqrt{K_p T_i}$.

By (3) it is possible to verify that the perturbation introduced by changes in the load power does not introduce steady-state errors in the dc-link voltage. Usually, the time constant of the dc voltage regulator is several times greater than that of the current controller. Thus, the two control loops can be designed as two independent systems.

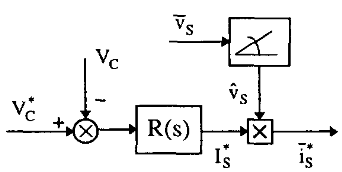

Fig. 3. Block diagram of the dc voltage regulator.

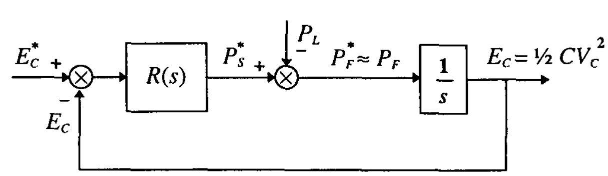

Fig. 4. Control loop of the capacitor energy

A. Control scheme based on the source current measurement

In this case, the control system acts in order to perform a direct regulation of the source currents, which must be sinusoidal and in phase with the corresponding line-to-neutral voltages. The voltage and current equations are

$$\bar{v}_S = \bar{v}_F + L\frac{d\bar{i}_F}{dt} \qquad (4)$$

$$\bar{i}_S = \bar{i}_F + \bar{i}_L\,. \qquad (5)$$

Being the rate of change of the filter current usually higher than that of the load current, (4) can be written as

$$\bar{v}_F = \bar{v}_S - L\frac{d\bar{i}_S}{dt}\,. \qquad (6)$$

For small variations, the time derivatives can be replaced by finite differences and (6) yields

$$\bar{v}_F = \bar{v}_S - \frac{L}{\Delta t}\Delta\bar{i}_S\,. \qquad (7)$$

Equation (7) is used to implement the control scheme shown in Fig. 5, where $\Delta\bar{i}_S$ represents the instantaneous source current error.

Under the assumptions made, and for an ideal PWM inverter, the transfer function of the ac current controller is

$$\bar{i}_S = \frac{1}{1+\tau_i s}\bar{i}_S^* + \frac{\tau_i s}{1+\tau_i s}\bar{i}_L, \quad \text{where} \quad \tau_i = L/K_i\,. \qquad (8)$$

The first term of (8) shows that the relationship between $\bar{i}_S^*$ and $\bar{i}_S$ is given by a low-pass filter with the time constant τ_i. High values of the ac-link inductance cause an increase of the time constant τ_i, but this effect can be compensated by adjusting the parameter K_i of the ac current regulator. The second term of (8) shows that the load current acts as a disturbance through a derivative network. As a consequence, the high order harmonics of the load current cannot be compensated by the active filter and will be reflected on the source current.

B. Control scheme based on the load current measurement

In this case, an indirect regulation of the source current is achieved by introducing a closed loop control of the "filter flux", defined as the time integral of the filter voltage. The block diagram representing the basic control principle used to generate the control signals for the inverter is shown in Fig. 6. The integration of (4) leads to the following "flux equation"

$$\bar{\varphi}_F^* = \bar{\varphi}_S - L\bar{i}_F^*\,, \qquad (9)$$

where $\bar{\varphi}_F^*$ is the reference "filter flux", and $\bar{\varphi}_S$ is the actual "source flux". The reference filter current is given by $\bar{i}_F^* = \bar{i}_S^* - \bar{i}_L$, where $\bar{i}_L$ is the measured load current and $\bar{i}_S^*$ is the reference source current.

The steady-state relationship $\bar{v}_S = j\omega\bar{\varphi}_S$ can be introduced in (9) yielding the following equation

$$\bar{\varphi}_F^* = \frac{\bar{v}_S}{j\omega} - L\bar{i}_F^*\,. \qquad (10)$$

Equation (10) has been used in the block diagram of Fig. 6 to calculate $\bar{\varphi}_F^*$. The actual value of $\bar{\varphi}_F$ is obtained by integrating the output filter voltage, which can be determined on the basis of the dc voltage V_C and the inverter switch states S_A, S_B, S_C. In this way, the use of additional wide bandwidth voltage transducers can be avoided.

Assuming that the PWM inverter is ideal, the transfer function of the ac current control loop, according to the block diagram shown in Fig. 6, is

$$\bar{i}_F = \frac{1}{1+\tau_\varphi s}\left(\bar{i}_F^* + \frac{\tau_\varphi}{L}\bar{v}_S\right), \quad \text{where } \tau_\varphi = 1/K_\varphi\,. \qquad (11)$$

The first term of (11) represents the low-pass filter action applied to $\bar{i}_F^*$. The second term is a perturbation term related to the source voltage, which determines an error in tracking the filter current. However, this term can be easily compensated by subtracting to $\bar{i}_F^*$ the quantity $\bar{v}_S \cdot \tau_\varphi / L$ which can be calculated at any instant. If a complete compensation is assumed, the following transfer function can be obtained for the source current

$$\bar{i}_S = \frac{1}{1+\tau_\varphi s}\bar{i}_S^* + \frac{\tau_\varphi s}{1+\tau_\varphi s}\bar{i}_L\,. \qquad (12)$$

The comparison between (12) and (8) shows that the dynamic performance concerning the source current regulation is the same for the two control schemes.

It can be noted that the implementation of the control scheme represented in Fig. 6 requires the knowledge of the ac-link inductance L. If the estimated inductance L^* is different from the actual inductance L, only a partial compensation of the second term in (11) can be achieved. As a conse-

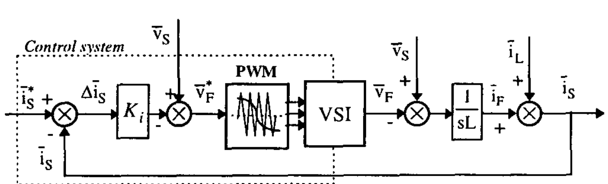

Fig. 5. Block diagram of the control system with PWM current regulator. The source current only is measured.

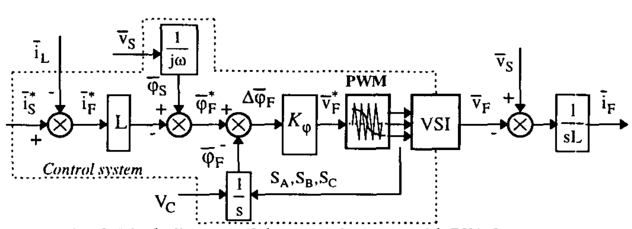

Fig. 6. Block diagram of the control system with PWM current regulator. The load current only is measured.

quence, an error between $\bar{i}_F$ and $\bar{i}_F^*$ will be introduced. In this case, the following transfer function for the filter current can be obtained

$$\bar{i}_F = \frac{L^*/L}{1+\tau_\varphi s}\bar{i}_F^* . \qquad (13)$$

It can be seen from (13) that an error in the estimation of L leads to a corresponding error in tracking $\bar{i}_F^*$. However, the behavior of the active filter is satisfactory even in presence of an error between $\bar{i}_F$ and $\bar{i}_F^*$. This because the outer dc voltage control loop acts in order to adjust the magnitude of $\bar{i}_S^*$ to a value compatible with the power balance equation.

IV. Numerical Results

The performance of the active filter configurations shown in Figs. 5 and 6 has been analyzed in steady-state and transient operating conditions. For this purpose, a numerical simulation of the whole power conditioning system has been carried out by using Simulink of Matlab. The assumptions of ideal sinusoidal source voltages (380 V, 50 Hz) and ideal inverter switches have been made. The steady-state performance has been verified considering a non-linear load constituted by a three-phase thyristor rectifier supplying a resistive-inductive load, controlled with a firing angle α=30°. Step changes have been applied to the load to investigate the dynamic behavior of the control system.

The simulation results are shown in Figs 7 and 8, for the control schemes based on the source current measurement and load current measurement, respectively. The results are related to the following data:

thyristor commutation time	600 µs,
switching frequency	10 kHz,
ac-line inductor parameters	L = 2 mH, R = 0.1 Ω,
dc-link reference voltage	V_C^* = 750 V,
dc-link capacitor	C = 1000 µF.

As can be seen in Figs. 7 and 8, during the first 40 ms the active filters are operating in steady-state conditions. Then, a step change of the load is applied determining an increase in the load current from 20 to 40 A. The behavior of the two control schemes is practically the same, leading to source currents with a low harmonic content and in-phase with the corresponding line-to-neutral voltages. After 80 ms the load is switched off, causing a temporary increase in the dc-link voltage. The reference value of dc-link voltage is recovered in about 20 ms for the control scheme with the source current measurement, and about 30 ms for that based on the load current measurement. It should be noted that the results given in Figs. 7 and 8 have been obtained using the same parameters for the dc voltage regulator. It has been also verified that the performance of the two control scheme is quite similar to that of standard schemes, which utilize two current measurement systems.

Numerical results in steady state and transient conditions

(a) - dc voltage, V_C **(b)** - line-to-neutral voltage, v_S **(c)** - load current, i_L **(d)** - compensated source current, i_S

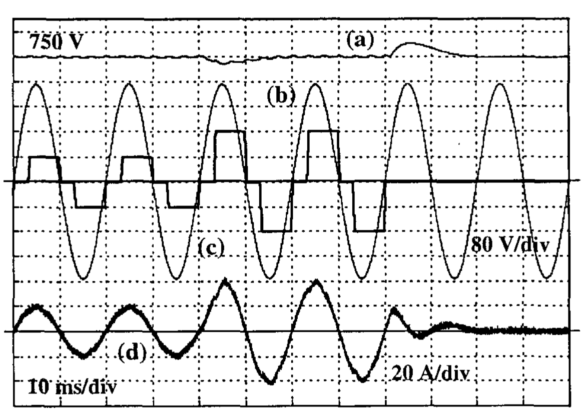

Fig. 7. Source current measurement only.
Load: thyristor rectifier, α=30°.

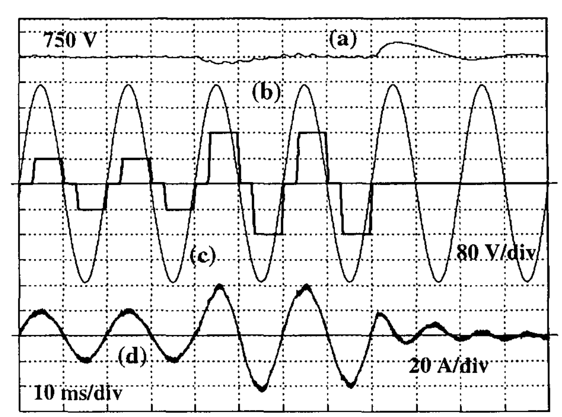

Fig. 8. Load current measurement only (flux method).
Load: thyristor rectifier, α=30°

V. EXPERIMENTAL TESTS

To validate the numerical simulations, the control system has been digitally implemented on a TMS320C31 DSP based board. As a first step in the experimental tests, the behaviour of the active filter configuration based on the measurement of the source currents (Fig. 5) has been investigated.

Fig. 9 shows the block diagram of the active filter used for the experimental tests. The IGBT VSI is shunt-connected to the 220 V, 50 Hz power grid by means of a 2 mH, 3-phase ac-link inductor. The dc-link capacitance is 1000 μF and the reference dc-link voltage is 450 V.

The active filter is shunt-connected to a three-phase, three-wires system. Thus, the sum of the line-to-line voltages is zero, and only two voltages (i.e. v_{Sab}, v_{Sbc}) are necessary to define the source voltage system. In the case of sinusoidal and balanced supply voltages, the three phase system can be defined by one line-to-line voltage (v_{Sab}) only. In the experimental setup the instantaneous value of v_{Sab} has been measured, and the line-to-neutral voltage vector $\bar{v}_S$ has been calculated by the DSP. The source voltage identification subsystem is represented by the dashed block a) in Fig. 9.

The synchronization with the source voltages has been realized by a digital Phase Locked Loop (PLL) algorithm. This algorithm needs to detect the zero crossing of v_{Sab}, then it quickly tunes the phase of v_{Sab}, giving the unity space vector $\hat{v}_S$ as output. The magnitude V_{SM} of $\bar{v}_S$ has been calculated on the basis of the RMS value of v_{Sab}.

The unity line-to-neutral voltage vector $\hat{v}_S$ has been also used to generate the reference source current $\bar{i}_S^*$, as shown in Fig. 3 and in the subsystem b) of Fig. 9. In particular, $\bar{i}_S^*$ has been calculated multiplying $\hat{v}_S$ by the reference source current magnitude I_S^* generated by the dc voltage regulator. The

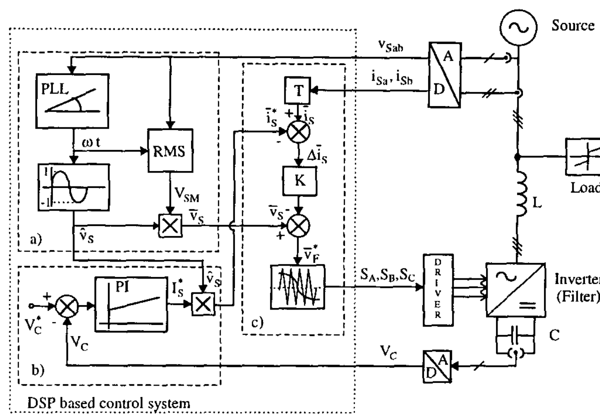

Fig. 9. Block diagram of the active filter used for experimental tests
a) source voltage identification subsystem
b) dc voltage regulator subsystem
c) current regulator subsystem

current regulator has been implemented in the subsystem c) of Fig. 9 according to the block diagram of Fig. 5. In order to synthesize the calculated output filter voltage $\bar{v}_F^*$, a triangular carrier PWM technique has been used to control the VSI.

The active power filter prototype has been firstly used to compensate the reactive power of a linear R-L load (cos φ = 0.8). The results obtained are shown in Fig. 10. As expected, the reactive power is compensated and the resulting source current is almost sinusoidal and in phase with the corresponding line-to-neutral voltage.

The harmonic compensation capability of the active filter has been tested connecting a full bridge diode rectifier (non-linear load) to the mains. The results are shown in Fig. 11. As expected, the load current harmonics disappear in the source current, with exception of the high order harmonics due to the fast current commutations.

Experimental results in steady-state condition

(a) - line-to-neutral voltage, v_S **(b)** - load current, i_L **(c)** - compensated source current, i_S

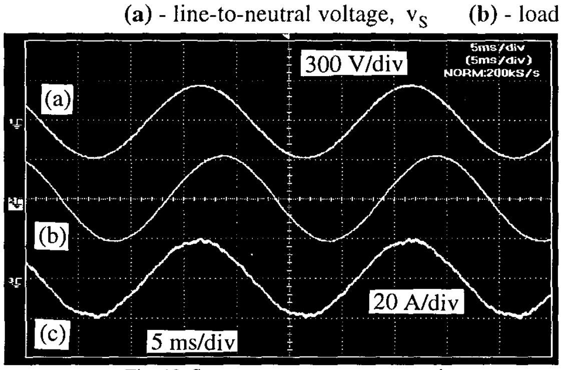

Fig. 10. Source current measurement only.
Load: R-L, cosφ = 0.8.

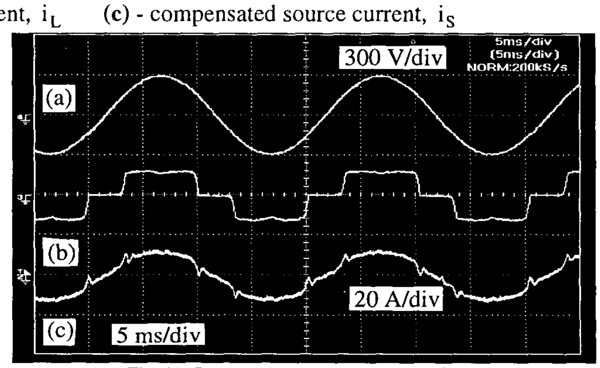

Fig. 11. Source current measurement only.
Load: full bridge diode rectifier

VI. Conclusions

Two control schemes for active power filters which impose sinusoidal source currents in phase with the corresponding line-to-neutral source voltages have been analyzed. The control techniques are based on a single current measurement system, leading to simple schemes which can be easily implemented. The current regulation is obtained by a PWM controlled VSI. Transfer functions are given to emphasize the dynamic response of both the dc voltage and ac current control loops. The numerical and experimental results have shown that the performance of the two control schemes is practically the same, giving sinusoidal source currents with unity power factor in both cases. The results obtained have clearly shown that, even using a single measurement system, the active filter performance is quite similar to that of standard solutions.

References

[1] L.Gyugyi, E.C.Strycula, "Active AC Power Filter," *Proc. IEEE-IAS Annual Meeting*, pp. 529, 1976.

[2] H.Akagi, Y.Kanazawa, A.Nabae, "Instantaneous Reactive Power Compensators Comprising Switching Devices without Energy Storage Components," *IEEE Trans. on IA*, Vol. 20, pp. 625, 1984.

[3] H.Akagi, A.Nabae, S.Atoh, "Control Strategy of Active Power Filters Using Multipole voltage-source PWM Converters," *IEEE Trans. on IA*, Vol. 22, pp. 460-465, May/June 1986.

[4] L.Malesani, L.Rossetto, P.Tenti, "Active Filters for Reactive Power and Harmonic Compensation," *Proc. IEEE-PESC*, pp. 321-330, June 1986.

[5] H.Fujita, H.Akagi, "The Unified Power Quality Conditioner: The Integration of Series Active Filter and Shunt Active Filters," *Proc. IEEE-PESC*, Baveno (IT), pp. 494-501, June 1996.

[6] S.Bhattacharya, D.M.Divan, B.Banerjee, "Synchronous Reference Frame Harmonic Isolator Using Series Active Filters," *Proc. EPE Conference*, Florence (IT), Vol. 3, pp. 30-35, September 1991.

[7] S.Bhattacharya, D.M.Divan, "Design and Implementation of a Hybrid Series Active Filter System," *Proc. IEEE-PESC*, Atlanta, 1995.

[8] V.Soares, P.Verdelho, G.Marques, "Active Power Filters Control Circuit Based on the Instantaneous Active and Reactive Current i_d-i_q Method," *Proc. IEEE-PESC*, pp. 1096-1108, June 1997.

[9] D.M.Brod, D.W.Novotny, "Current Control of VSI-PWM Inverters," *IEEE Trans. on IA*, Vol. 21, No.4, 562-570, May/June 1985.

[10] A.Nabae, S.Ogasawara, H.Akagi, "A Novel Control Scheme for Current Controlled PWM Inverters," *IEEE Trans. on IA*, Vol. 2, No.4, pp. 697-701, 1986.

[11] S.Bhattacharya, G.H.Holmes, D.M.Divan, "Optimizing Three Phase Current Regulators for Low Inductance Loads," *Proc. IEEE-IAS*, 1995.

[12] I.W.Rowan, R.J.Kerkman, "A New Synchronous Current Regulator and an Analysis of Current Regulated PWM Inverters," *IEEE Trans. on IA*, Vol. 22, No.4, pp. 678-690, 1996.

[13] S. Bhattacharya, A. Veltman, D.M. Divan, R.D. Lorenz, "Flux Based Active Filter Controller," *Proc. IEEE-IAS*, pp. 2483-2491, 1995.

[14] S.Fukuda, T.Endoh, "Control Method and Characteristics of Active Power Filters," *Proc. EPE Conf.*, Brighton (UK), pp. 139-144, 1993.

[15] P.Delarue, R.Bausierre, "New Control Methods for Active Power Filter Needing Line Current Measurements only," *Proc. EPE Conf.*, Sevilla (SP), Vol. 1, pp. 914-919, 1995.

[16] J.Dixon, J.Contardo, L.Moran, "DC Link Fuzzy Control for an Active Power Filter, Sensing the Line Current Only ", *Proc. IEEE-PESC*, Vol. 2, pp. 1109-1114, 1997.

[17] U. Reggiani, D. Casadei, G. Grandi, "Active Power Filters Based on a Single Current Measurement System" , *SPEEDAM Conference*, Sorrento (IT), June 1998.

[18] D. Casadei, G. Grandi, U. Reggiani, G. Serra: "Analysis of a Power Conditioning System for Superconducting Magnetic Energy Storage", *IEEE-ISIE Conference*, Pretoria (SA), July 7-10, 1998.